• **Basic Research** •

Anti-proliferation and apoptosis-inducing effects of sodium aescinate on retinoblastoma Y79 cells

Lei Li[1], Bing Xu[1,2], Cai–Rui Li[3], Miao–Miao Zhang[1], Sheng–Jun Wu[1], Wen–Jun Dang[1], Jing–Chen Liu[1], Shu–Guang Sun[4], Wei Zhao[3]

[1]College of Clinical Medicine, Dali University, Dali 671000, Yunnan Province, China
[2]Department of Ophthalmology, Fuling Central Hospital of Chongqing City, Fuling 408000, Chongqing Province, China
[3]Department of Ophthalmology, the First Affiliated Hospital of Dali University, Dali 671000, Yunnan Province, China
[4]Department of Endocrinology, the First Affiliated Hospital of Dali University, Dali 671000, Yunnan Province, China
Co-first authors: Lei Li and Bing Xu
Correspondence to: Cai-Rui Li. Department of Ophthalmology, the First Affiliated Hospital of Dali University, Dali 671000, Yunnan Province, China. lcrbrett@163.com; Shu-Guang Sun, Department of Endocrinology, the First Affiliated Hospital of Dali University, Dali 671000, Yunnan Province, China. sshuglily@163.com.
Received: 2020-03-10   Accepted: 2020-07-16

Abstract

● **AIM:** To investigate the anti-proliferation and apoptosis-inducing effects of sodium aescinate (SA) on retinoblastoma Y79 cells and its mechanism.

● **METHODS:** Y79 cells were cultured at different drug concentrations for different periods of time (24, 48, and 72h). The inhibitory effect of SA on proliferation of Y79 cells was detected by the cell counting kit-8 (CCK-8) assay, and the morphology of Y79 cells in each group was observed under an inverted microscope. An IC50 of 48h was selected for subsequent experiments. After pretreatment with SA for 24 and 48h, cellular DNA distribution and apoptosis were detected by flow cytometry. Real-time qunatitative polymerase chain reaction (RT-qPCR) and Western blot were used to assess changes in related genes (CDK1, CyclinB1, Bax, Bcl-2, caspase-9, caspase-8, and caspase-3).

● **RESULTS:** SA inhibited proliferation and induced apoptosis of Y79 cells in a time-dependent and concentration-dependent manner. Following its intervention in the cell cycle pathway, SA can inhibit the expression of CDK1 and CyclinB1 at the mRNA and protein levels, and block cells in the G2/M phase. In caspase-related apoptotic pathways, up-regulation of Bax and down-regulation of Bcl-2 caused caspase-9 to self-cleave and further activate caspase-3. What's more, the caspase-8-mediated extrinsic apoptosis pathway was activated, and the activated caspase-8 was released into the cytoplasm to activate caspase-3, which as a member of the downstream apoptotic effect group, initiates a caspase-cascade reaction that induces cell apoptosis.

● **CONCLUSION:** SA inhibits the proliferation of Y79 cells by arresting the cell cycle at the G2/M phase, and induces apoptosis *via* the caspase-related apoptosis pathway, indicating that SA may have promising potential as a chemotherapeutic drug.

● **KEYWORDS:** sodium aescinate; retinoblastoma; intrinsic apoptosis pathway; extrinsic apoptosis pathway; cell cycle arrest

INTRODUCTION

Retinoblastoma, an invasive intraocular cancer originating in the photoreceptor cell layer of the retina, accounts for 4% of malignant tumors in children. The main clinical manifestations of retinoblastoma are white pupil and strabismus[1-2]. Although early diagnosis and effective treatment are highly curative, delayed diagnosis, rapid progression, metastasis and limited treatment methods often lead to blindness and even death[3]. Current methods of treatment mainly include chemotherapy, local treatment (such as cryotherapy and laser photocoagulation) and surgical treatment[4]. But these treatments have adverse consequences such as drug resistance, serious toxic and adverse effects, and poor survival quality for children. Therefore, it is a matter of urgency to find an effective drug that can improve the prognosis in children.

Sodium aescinate (SA), a natural mixture of triterpenoid saponins, has antioxidant, anti-exudation, edema reduction and vascular protection effects[5-6], and demonstrates good clinical tolerance. In recent several years, many researchers have

manifested that SA can play an anti-tumor role in a number of tumor cells by inducing apoptosis and cell cycle arrest[7-12]. Moreover, SA, as a member of natural medicinal plants, may have potential as a high-efficiency and low-toxicity anti-cancer drug. However, the inhibitory effect of SA on retinoblastoma cells has not been studied.

The effect of apoptosis is extremely important in the normal development of the body and the accomplishment of various physiological functions. Tumor cells can escape apoptosis, an ability that leads to the occurrence and development of cancer[13]. Therefore, inducing apoptosis of cancer cells is a strategy of antineoplastic treatments. Caspase plays a central role in the control and execution of apoptosis[14]. Mitochondria, when activated, can mediate two apoptotic pathways to execute apoptotic instructions, including caspase-dependent intrinsic and extrinsic pathways[15]. In addition, the modern view is that cancer is a cell cycle disease. Previous studies have shown that almost all the products of oncogenes and tumor-suppressor genes are directly or indirectly involved in cell cycle regulation. Previous studies have interpreted that almost all oncogenes and tumor suppressor genes play direct or indirect roles in the regulation of the cell cycle. Mutations in these genes can lead to uncontrolled cell cycle, excessive cell growth, and eventual tumor formation. In terms of cell cycle and apoptosis, however, the effects of SA on retinoblastoma has not been covered.

In this study, therefore, we demonstrated the anti-proliferation and apoptosis-inducing effects of SA on human retinoblastoma Y79 cells. We also propose a possible mechanism whereby SA induces cell cycle arrest and apoptosis.

MATERIALS AND METHODS

Cell Culture and Sodium Aescinate Preparation RPMI 1640 full-medium (containing 10% fetal bovine serum, 1% penicillin, and 1% streptomycin) was used to culture Y79 cells (Beijing Baina Co., Ltd.) in an incubator at 37℃, with 5% CO_2. SA (in which the content of aescin A was 33.5%, aescin B was 31.4%, aescin C was 17.8% and aescin D was 14.2%) was prepared in RPMI 1640 complete medium and diluted to the appropriate concentration for further use. After the addition of SA solution (0, 40, 60, 80, and 100 µg/mL) to Y79 cells, the cells were incubated for 24, 48, and 72h, and then cell counting kit-8 (CCK-8) assay was carried out. Next, flow cytometry was performed after treatment with 35 µg/mL SA for 24h and 48h. Finally, the cells were treated with 35 µg/mL SA for 48h and then subjected to Western blot and fluorescent real-time quantitative polymerase chain reaction (RT-qPCR) analysis.

Cell Viability Assay The cultured cells were categorized as the SA group, the SA control group (in which interference with drug absorbance was removed), a control group, and a blank group. CCK-8 method was used to examine cell viability,

as follows: cell suspension of $1×10^5$/mL was prepared, 100 µL of each well was inoculated in 96-well plate and cultured overnight. SA was added, at a series of concentrations (0, 40, 60, 80, and 100 µg/mL) to the culture medium for 24, 48, or 72h, using 5 wells per concentraction. CCK-8 agentia (20 µL) was then added to each well for 2-4h. Optical density (OD) values were measured by a spectrophotometer at a wavelength of 450 nm. Data are reported as percentages of cell viability, percentages in control cells considered as 100%:

Cell viability=[OD$_{(SA)}$−OD$_{(SA-control)}$/[OD$_{(control)}$−OD$_{(blank)}$]×100%

Morphological Changes Prior to the addition of CCK-8 reagent, morphological changes in Y79 cells were observed under an inverted microscope (200×) and photographed.

Cell Cycle Assay Y79 cells were seeded in 6-well plates and incubated for 24h or 48h with 35 µg/mL SA. They were then collected, fixed with 70% precooled ethanol, and overnight at 4℃. Following staining with 500 µL propidium iodide (PI) solution consisting of a mixture of 500 µL staining buffer, 25 µL PI solution and 10 µL RNaseA, the cells were collected, suspended, and bathed at 37℃ for 30min in dark. Cell analysis was then performed by means of a NovoCyte flow cytometer (ACEA Biosciences, Inc., USA).

Cell Apoptosis Assay For analysis of apoptosis, Y79 cells were cultured with 60 µg/mL SA for 24 or 48h. Apoptosis detection was carried out in accordance with Annexin V-FITC kit instructions and was analyzed using the NovoCyte flow cytometer.

RT-qPCR Assay According to the instructions, total RNA was extracted and reverse transcriptional reaction was conducted to obtain cDNA for use. RT-qPCR was performed using the ChamQ SYBR qPCR Master Mix kit (Nanjing, China) on a StepOnePlus RT-qPCR detection system (ThermoFisher Scientific, USA). The primer sequences were as recorded in Table 1. Its reaction conditions were 95℃ for 3min, 95℃ for 15s, 55℃ for 30s, with 30 cycles in total. The $2^{-\Delta\Delta Ct}$ method was used to calculate relative gene expression levels.

Western Blot Assay The total protein was extracted, and its concentration was determined. Each protein was diluted to the same concentration and denatured in boiling water bath for later use. The 12% sodium dodecyl sulfate polyacrylamide gel electrophoresis (SDS-PAGE) was prepared, 20 µg samples were taken from SA group and control group separately, and protein marker 5 µL was used for electrophoresis. The gel was cut according to the size of the target strip, and the PVDF membrane was transferred by semi-dry transfer machine (Bio-rad, USA). The membrane was sealed by 5% skim milk at room temperature for 1h. Tris-buffered saline Tween-20 (TBST) buffer was washed routinely and incubated at 4℃ overnight with primary antibodies anti-Bax, anti-Bcl-2, anti-

Table 1 Primer pairs used for RT-qPCR

Gene	Primer pair sequences (5'-3')	GenBank Accession No.
β-actin	F: CTGGGACGACATGGAGAAA R: GCACAGCCTGGATAGCAAC	NM_001101.3
CDK1	F: GATTCTATCCCTCCTGGTCAGT R: CAGCCAGTTTAATTGTTCCTTT	NM_001786.4
CyclinB1	F: GTCGGGAAGTCACTGGAAAC R: AACCGATCAATAATGGAGACAG	NM_031966.3
Bax	F: TTGCTTCAGGGTTTCATCC R: CGCTCAGCTTCTTGGTGG	NM_138761.3
Bcl-2	F: CGCTGGGAGAACAGGGTA R: GGGCTGGGAGGAGAAGAT	NM_000633.2
Caspase-3	F: GGTTCATCCAGTCGCTTTG R: ATTCTGTTGCCACCTTTCG	NM_032991.2
Caspase-8	F: TTCCTGAGCCTGGACTACATT R: GAAGTTCCCTTTCCATCTCCT	NM_001228.4
Caspase-9	F: ACTAACAGGCAAGCAGCAAA R: CCAAATCCTCCAGAACCAAT	NM_001229.4

caspase-3, anti-caspase-8, anti-caspase-9, anti-CDK1, and anti-CyclinB1 (diluted at 1:1000; Cat. #5023; Cat. #15071; Cat. #14220; Cat. #4790; Cat. #9508; Cat. #28439; Cat. #4135; CST, Inc.), and anti-β-actin (diluted at 1:1000; Cat. #AF003; Beyotime Biotechnology). This was followed by incubation at normal temperature for 1.5h with HRP-conjugated antibody (diluted at 1:1000; Cat. #A0208 and Cat. #A0216; Beyotime Biotechnology). Immunoreactivity strips were visualized using an enhanced chemiluminescence system (Beyotime Biotechnology) and the densitometry of the strips was determined with Image J software.

Statistical Analysis Data were expressed as means±standard deviation (SD) of 3 independent experiments. Statistical analysis was conducted by using GraphPad Prism 7.0 or SPSS 21.0. Unpaired Student's t-tests (two-tailed) or one-way ANOVA analysis were used to compare control and SA groups. $P<0.05$ is shown significant difference.

RESULTS

Inhibitory Effects of SA on Y79 cells To detect the inhibitory effect of SA on Y79 cells, the cells were cultivated with 40, 60, 80 or 100 μg/mL of escin sodium for 24, 48, and 72h, and then subjected to CCK-8 assays (Table 2). Compared to control, Y79-cell viability was significantly inhibited by SA treatment at 24, 48, and 72h, separately ($P<0.01$). The inhibitory effect of SA on Y79 cells is time and concentration dependencies. After treatment, we viewed the cell morphology under an inverted microscope in order to see the inhibitory effect clearly. As shown in Figure 1, with increasing SA concentration and time, the number of Y79 cells decreased, a small number of Y79 cells were formed into clusters, irregular shape, while cell debris increased. Cells in the control group remained in good condition, with clear outlines, and they stuck to the medium like grape clusters.

Table 2 Viability of Y79 cells after SA treatment mean±SD, $n=3$

Groups	Concentration (μg/mL)	Cell viability (%)		
		24h	48h	72h
Control	-	100.00±1.89	100.00±3.21	100.00±7.25
SA	40	73.78±12.02	34.47±0.61[b]	21.26±3.79[b]
	60	37.93±1.30[b]	19.55±1.43[b]	12.55±0.75[a]
	80	73.78±12.02[b]	15.35±0.42[b]	12.02±0.09[a]
	100	33.19±0.50[b]	14.83±0.29[b]	11.46±1.05[a]

[a]$P<0.01$; [b]$P<0.001$ *vs* control group.

SA Inhibits Cell Proliferation in Y79 Cells by Arresting the Cell Cycle at G2/M Phase To find out whether SA induces inhibition of proliferation and blockage of the cell cycle, we used flow cytometry to analyze cell cycle distribution. In Figure 2A-2C, in the G2/M phase, compared with the control group, the proportion of cells in the SA group increased remarkably ($P<0.01$). This caused a time-dependent increase in the G2-phase cell population (24.34%±0.27% and 9.48%±0.48% for 24h and 48h of SA group, respectively, compared with 21.04%±0.11% and 2.41%±0.80%, respectively, for the control group), and was accompanied by a decrease in cell populations at S phases ($P<0.01$). To further elucidate the mechanism underlying G2/M arrest, RT-qPCR and Western blot were adopted to examine the levels of the regulatory genes (CDK1 and CyclinB1) at the G2/M phase. As shown in Figure 2D, CDK1 was obviously down-regulated at the mRNA level. Meanwhile, at the protein level, both CDK1 and CyclinB1 expression were significantly decreased after being treated with SA compared to the control group (Figure 2E and 2F). These data manifested that SA efficiently blocks the G2/M phase by inhibiting the expression of CDK1 and CyclinB1.

SA Induces Apoptosis in Y79 Cells Annexin V-FITC/PI staining enabled us to find out a significant rate of apoptosis.
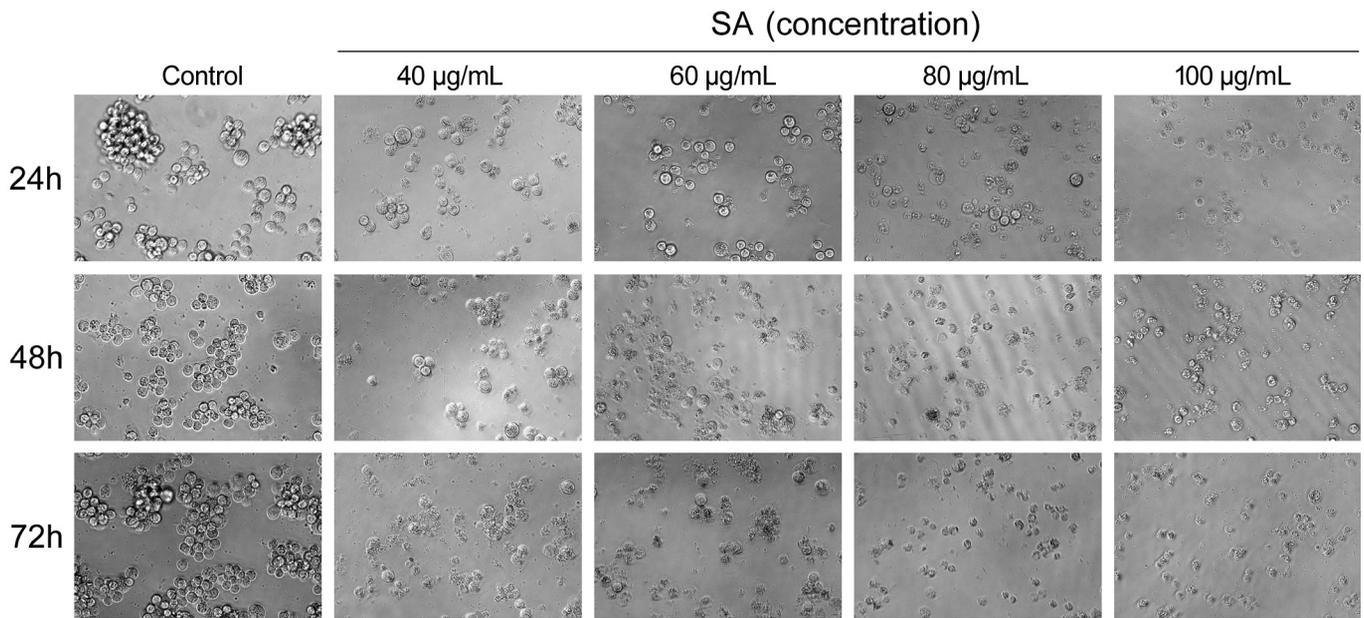
Figure 1 Morphology of Y79 cells after treatment with different concentrations of SA for 24, 48, and 72h.
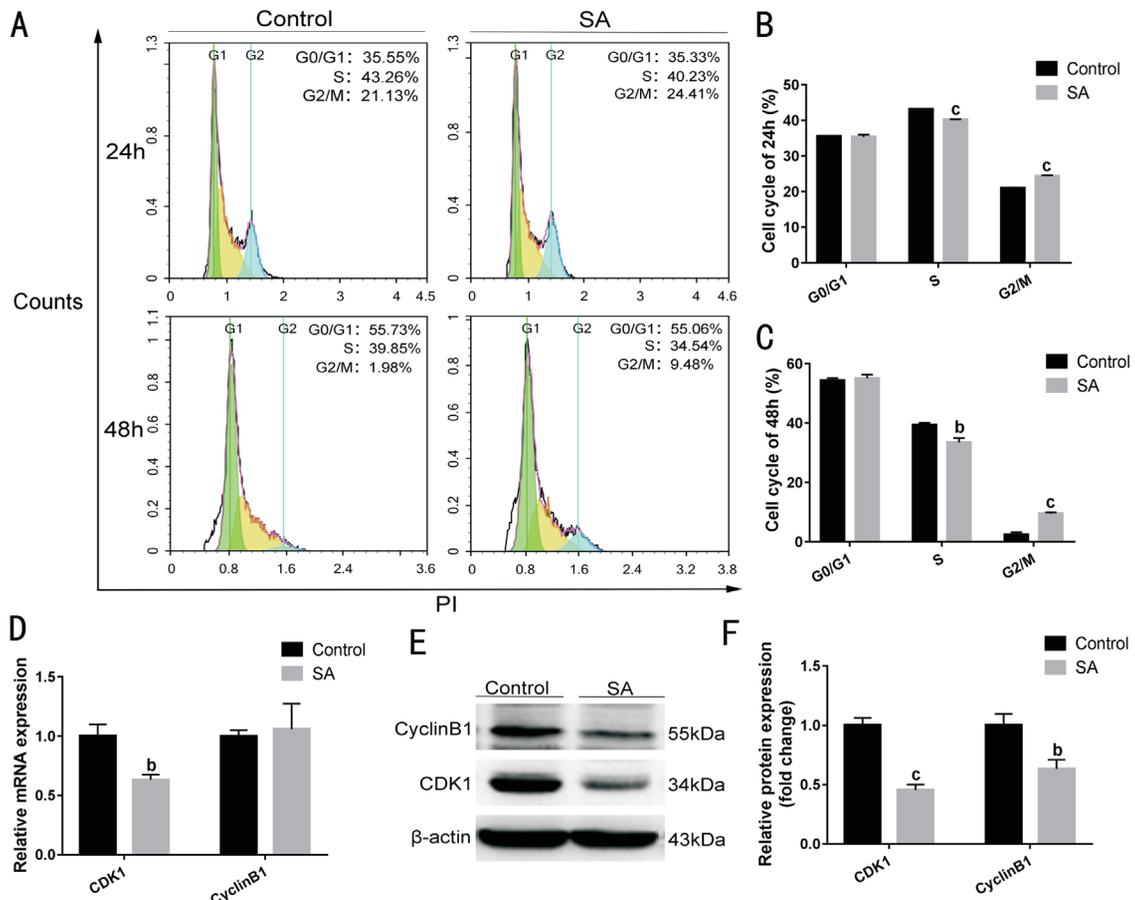

Figure 2 SA inhibits the proliferation of Y79 cells by preventing the cell cycle in G2/M phase A: Cell cycle distribution in Y79 cells following their incubation in the control and the SA groups for 24h and 48h was assessed by flow cytometry; B, C: Histogram showing cell cycle distribution after 24 and 48h, respectively; D: Expression levels of CDK1 and CyclinB1 in Y79 cells, detected by qRT-PCR assay after treatment with SA (35 μg/mL) for 48h; E: Expression levels of CDK1 and CyclinB1 in Y79 cells, detected by Western blot assay; F: Histogram compares relative protein expression levels of CDK1 and CyclinB1. [b]$P<0.01$ and [c]$P<0.001$ *vs* control.

Also, as shown in Figure 3A and 3B, after being treated with 35 μg/mL SA for 24 and 48h, the percentage of apoptosis were 15.27%±1.46% and 16.87%±0.83%, the control group were 2.21%±0.14% and 4.42%±0.26% respectively. The difference was statistically significant (all $P<0.01$). These results indicate that SA effectively induced Y79 cell apoptosis.
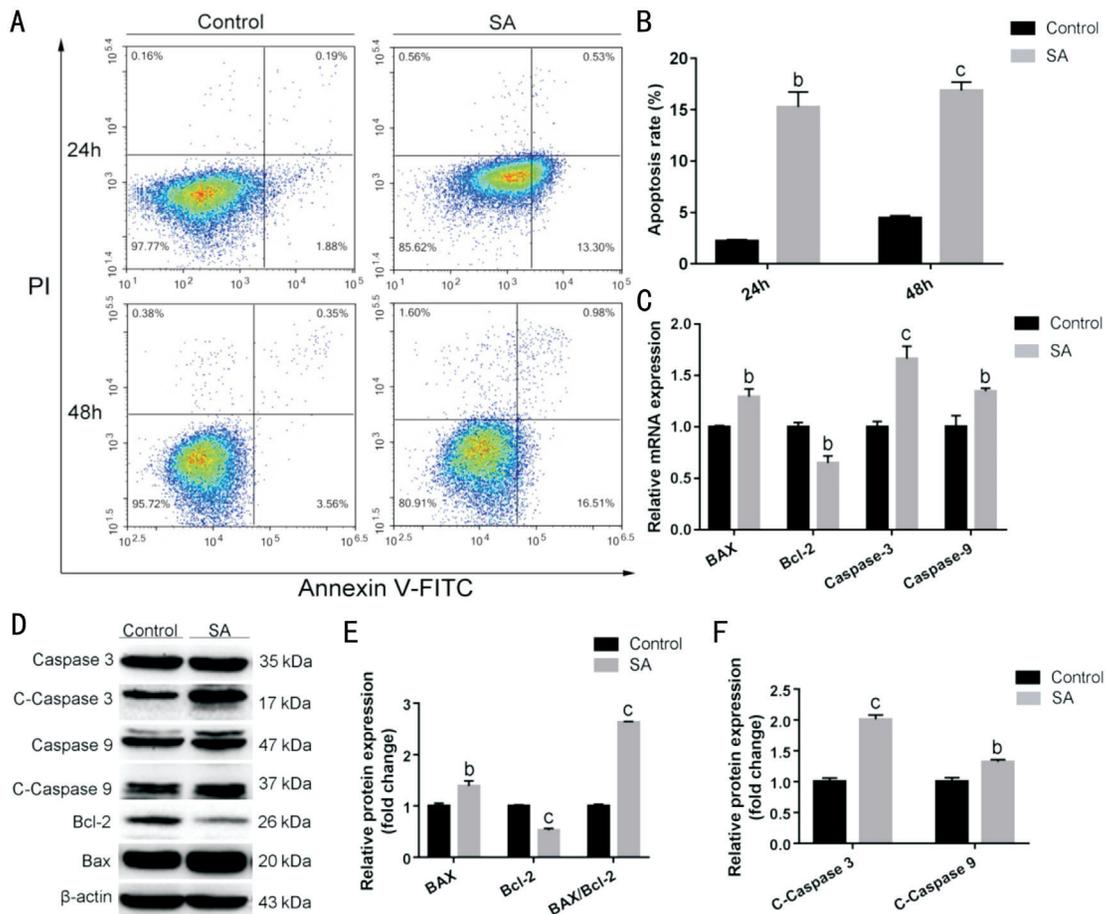
Figure 3 Intrinsic pathway involved in SA-induced apoptosis in Y79 cells A: Flow cytometry demonstrates changes over time (24 and 48h) in Y79-cell apoptosis in the control and the SA group; B: Changes in Y79-cell apoptosis rate in the control group and after SA treatment for 24 and 48h; C: The expression levels of Bax, Bcl-2, caspase-3, and caspase-9 in Y79 cells, detected by RT-qPCR assay after treatment with SA (35 μg/mL) for 48h; D: In Western blot assay, the protein expression levels of caspase-3, cleaved-caspase 3, caspase-9, cleaved-caspase-9, Bcl-2, and Bax in Y79 cells; E: Comparison of Bax and Bcl-2 protein expression and Bax/Bcl-2 ratio; F: Comparison of cleaved-caspase-3 and cleaved-caspase-9 protein expression. The expression level of β-actin is considered as one. [b]$P<0.01$ and [c]$P<0.001$ *vs* control.

Intrinsic Pathway Involved in SA-induced Apoptosis Here we further investigated the mechanism underlying the induced apoptosis. Following SA treatment, in Figure 3C, the expressions of Bax, caspase-9, and caspase-3 at the mRNA level were up-regulated compared to the control group, whereas Bcl-2 was down-regulated. Furthermore, Western blot showed that Bax, cleaved-caspase-9, and cleaved-caspase-3 increased, while the expression of Bcl-2 decreased in Y79 cells treated with SA (in all cases $P<0.01$; Figure 3D-3F). They are key regulatory components involved in apoptosis. As a result, the decrease in Bcl-2 expression and the increase in Bax expression in Y79 cells resulted in an increase in the ratio Bax/Bcl-2 (Figure 3E). The intrinsic apoptosis pathway was then activated by caspase-9, finally activating the apoptotic effector caspase-3, which induced Y79-cell apoptosis.

Extrinsic Pathway Involved in SA-induced Apoptosis Expression of additional genes was also detected in extrinsic apoptotic pathways. In Figure 4A, higher expression of caspase-8 and caspase-3 was observed at the mRNA level

($P<0.001$). After Y79 cells were treated with SA for 48h, caspase-8 was cleaved into subunits and self-activated, the protein expression of cleaved caspase-8 increased ($P<0.001$, Figure 4B and 4C). What's more, the high cleaved caspase-3 expression together illustrated that SA-induced apoptotic cell death was performed by the extrinsic pathway.

DISCUSSION
Apoptosis is a major control mechanism and an important means of controlling cell number and proliferation[16]. Research in recent years has shown that SA is effective against a variety of tumors[17]. Our study suggested that SA can promote the occurrence of apoptosis and proliferation inhibition of retinoblastoma Y79 cells *in vivo*. The CCK-8 assay explained that SA has an anti-proliferative effect on Y79 cells and induces apoptosis in a time-dependent and concentration-dependent manner (Table 2). It is currently believed that selective induction of tumor cell apoptosis is one of the important mechanisms of tumor therapy. Therefore, after applying the CCK-8 assay to verify its anti-retinoblastoma
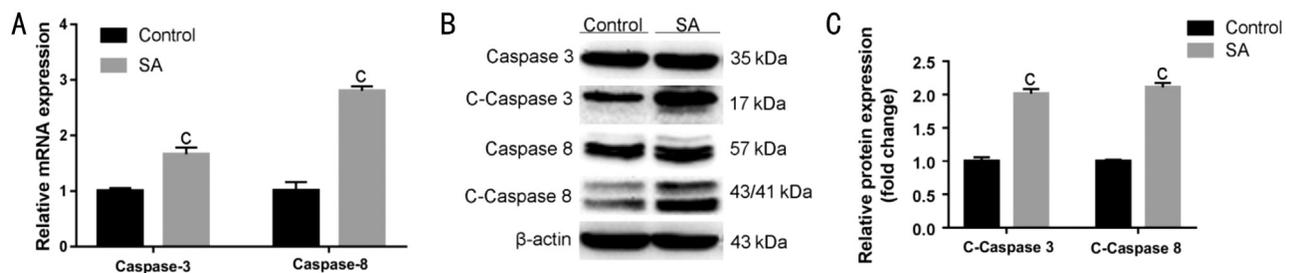
Figure 4 Extrinsic pathway involved in SA-induced apoptosis in Y79 cells A: mRNA expression levels of caspase-3 and caspase-8 in Y79 cells after treatment with SA (35 μg/mL) for 48h; B: Protein expression levels of caspase-3, cleaved-caspase-3, caspase-8, and cleaved-caspase-8 in Y79 cells; C: Comparison of cleaved-caspase-3 and cleaved-caspase-8 protein expression. [c]$P<0.001$ *vs* control.

properties, we further explored its mechanism of action on retinoblastoma, in order to provide a theoretical basis for its therapeutic use in the clinic.

Checkpoint is an important regulatory node in the cell cycle. The process of cell proliferation encounters at least two major checkpoints in the cell cycle, namely G1/S and G2/M[18]. Only by passing checkpoint tests can cells enter the next cell cycle[19]. Researches has shown that SA induces cell cycle arrest or apoptosis in a variety of cancer cells[20-24]. Here we showed that SA has a vital impact on cell distribution in the cell cycle: it notably decreased the DNA content in the S phase and blocked Y79 cells in the G2/M phase (Figure 2A-2C). In an attempt to understand the mechanism of SA-induced G2/M arrest, we analyzed the expression of CDK1 and CyclinB1- the G2/M checkpoint regulators. In the G2 phase, CyclinB1 and CDK1 formed the mature promoting factor (MPF) complex, which causes chromosome concentration, nuclear membrane rupture and spindle formation, and also initiates mitosis, promoting G2/M phase conversion and accelerating the cell cycle process[25]. Following SA treatment, the protein expression of CDK1 and CyclinB1 in Y79 cells was lower than that in control group (Figure 2E and 2F), and the synthesis of the MPF complex was reduced, leading to cell cycle arrest in the G2/M phase and preventing Y79 cells containing damaged DNA from entering mitosis. Our results suggested that the inhibition of Y79 cell proliferation is associated with cell cycle arrest in the G2/M phase, a molecular mechanism for commonly used anti-cancer drugs[18]. These results thus suggested that SA may be a potential drug against retinoblastoma.

The Bcl-2 protein family has been shown to play a critical role in the regulation of apoptosis. Members of the Bcl-2 family include two types: anti-apoptotic proteins (Bcl-2, Bcl-xl) and pro-apoptotic proteins (Bax, Bak, and others). It is generally believed that the anti-apoptotic Bcl-2 members can promote the survival of tumor cells by binding to members of the pro-apoptotic Bcl-2 family, thereby preventing activation of mitochondrial outer membrane melamination (MOMP) and cytotoxic caspase[26-27]. Studies have confirmed that when cells are damaged the pro-apoptotic BH3 protein serves as a death-

signaling sensor, activating multidomain proteins such as Bax and Bak, which can trigger MOMP and activate caspase to play a pro-apoptotic role by inserting itself into the mitochondrial membrane. Anti-apoptotic proteins directly inhibit MOMP by blocking the activation and activity of Bax/Bak[28]. Ultimately, the balance of antagonistic activity of the Bcl-2 family, expressed as the Bax/Bcl-2 ratio, determines whether MOMP and cell death[26-27,29]. After treatment with SA, Bax was higher than the control group at the mRNA and protein levels, while Bcl-2 was lower (Figure 3C-3E). It follows that the ratio of Bax/Bcl-2 was increased, exhibiting a pro-apoptotic effect. Bax located in the cytoplasm can sense the release of calcium ions in the endoplasmic reticulum, and translocates them to the mitochondria, where they form pores to increase the permeability of the mitochondrial membrane. This can help release cytochrome C into the cytoplasm, activate the mitochondrial apoptosis pathway[30], and undergo cleavage of genomic DNA[31] which leads to irreversible apoptosis of Y79 cells[32].

Apoptosis is the physiological process of removing unwanted or damaged cells. Mitochondria are the executors of cell survival and death. When stimulated by damage to DNA, ultraviolet light or chemotherapeutic drugs, mitochondria-dependent apoptosis pathways become activated and release some proteins from the mitochondrial intermembrane space. For example, cytochrome C, which binds to Apaf-1 and caspase-9 to form apoptotic bodies. These induce permeability of the mitochondrial outer membrane and activation of downstream caspase-9, which assists in the death of apoptotic cells by cleaving their own protein subsets[33-35]. In our study, AnnexinV-FITC/PI staining showed that SA induces apoptosis of Y79 cells (Figure 3A and 3B). Under the inverted microscope, Y79 cells showed morphological changes characteristic of apoptosis (Figure 1). We observed some such changes, including their numbers decreasing as they gradually loosened into a single floating, irregular shape, while cell debris increased. To further understand the mechanism of apoptosis, we used RT-qPCR and Western blot assays for verification. In PCR analysis, the expression of caspase-3 and caspase-9 were observably

up-regulated (Figure 3C). Western blot results showed that, compared with the control group, the expression of cleaved-caspase-9 and cleaved-caspase-3 in the SA group showed the same trend (Figure 3D and 3F). We speculated that SA causes cell damage in retinoblastoma cells, leading to upregulation of Bax and downregulation of Bcl-2, increasing permeability of the mitochondrial membrane, releasing cytochrome C from the mitochondrial membrane space into the cytoplasm, and binding Apaf-1 to form apoptotic complexes[36-37]. Caspase-9 was recruited into the apoptotic complex, became activated, and underwent autocatalytic cleavage. Furthermore, the cleavage unit of caspase-9 activated the downstream caspase-3, which then induced the caspase cascade to execute the apoptotic instructions[32,38-39].

Caspase-3 is the ultimate effector protein of apoptosis in the death-receptor apoptotic pathway. Caspase-3 is activated by an upstream promoter, such as caspase-8. Upstream of caspase-8 the Fas ligand (FasL or CD95L) binds to the Fas receptor (CD95) to form the death-domain protein, and to caspase-8 to form the death-inducible signaling complex, thereby triggering the activation of caspase-8, activating the downstream effector protein caspase-3, and inducing apoptosis[40]. In this study, we demonstrated that SA treatment can up-regulate the mRNA levels of caspase-3 and caspase-8 (Figure 4A), as well as the expression of cleaved caspase-8 and cleaved caspase-3 proteins (Figure 4B and 4C). Our results thus showed that SA can induce apoptosis of Y79 cells *via* an extrinic apoptosis pathway.

This study has certain shortcomings. In the future, animal studies should also be conducted, using the retinoblastoma xenograft model to evaluate the anti-tumor effect of SA and further explore other possible anti-tumor mechanisms. In conclusion, our results suggest that SA inhibits the proliferation and promotes the apoptosis of Y79 cells. In addition, SA down-regulates the expression of CDK1 and CyclinB1, and reduces MPF production, causing the cell cycle to stop in the G2/M phase. Furthermore, SA induces apoptosis of Y79 cells through the mitochondrial apoptotic pathway mediated by caspase-9 and through the death-receptor pathway mediated by caspase-8. These results lay a solid foundation for the development of SA as an effective chemotherapeutic drug for the treatment of retinoblastoma.

ACKNOWLEDGEMENTS

Conflicts of Interest: Li L, None; **Xu B,** None; **Li CR,** None; **Zhang MM,** None; **Wu SJ,** None; **Dang WJ,** None; **Liu JC,** None; **Sun SG,** None; **Zhao W,** None.

REFERENCES

1 Yang G, Fu Y, Zhang LX, Lu XY, Li QM. miR106b regulates retinoblastoma Y79 cells through Runx3. *Oncol Rep* 2017;38(5): 3039-3043.

2 Agnieszka B, Cezary G. Retinoblastoma. *Journal of Education, Health and Sport* 2018;8(7):204-213.

3 Mattosinho CCS, Moura ATMS, Oigman G, Ferman SE, Grigorovski N. Time to diagnosis of retinoblastoma in Latin America: a systematic review. *Pediatr Hematol Oncol* 2019;36(2):55-72.

4 Dimaras H, Kimani K, Dimba EA, Gronsdahl P, White A, Chan HS, Gallie BL. Retinoblastoma. *Lancet* 2012;379(9824):1436-1446.

5 Matsuda H, Li Y, Yoshikawa M. Effects of escins Ia, Ib, IIa, and IIb from horse chestnuts on gastrointestinal transit and ileus in mice. *Bioorg Med Chem* 1999;7(8):1737-1741.

6 Patlolla JM, Raju J, Swamy MV, Rao CV. Beta-escin inhibits colonic aberrant crypt foci formation in rats and regulates the cell cycle growth by inducing p21(Waf1/cip1) in colon cancer cells. *Mol Cancer Ther* 2006;5(6):1459-1466.

7 Hou H, Li WX, Cui X, Zhou DC, Zhang B, Geng XP. CARMA3/NF-κB signaling contributes to tumorigenesis of hepatocellular carcinoma and is inhibited by sodium aescinate. *World J Gastroenterol* 2019;25(36):5483-5493.

8 Wang XH, Xu B, Liu JT, Cui JR. Effect of beta-escin sodium on endothelial cells proliferation, migration and apoptosis. *Vascul Pharmacol* 2008;49(4-6):158-165.

9 Zhang ZZ, Gao J, Cai XT, Zhao YL, Wang YF, Lu WG, Gu ZH, Zhang SQ, Cao P. Escin sodium induces apoptosis of human acute leukemia Jurkat T cells. *Phytother Res* 2011;25(12):1747-1755.

10 Güney G, Kutlu HM, Işcan A. The apoptotic effects of escin in the H-Ras transformed 5RP7 cell line. *Phytother Res* 2013;27(6): 900-905.

11 Shen DY, Kang JH, Song W, Zhang WQ, Li WG, Zhao Y, Chen QX. Apoptosis of human cholangiocarcinoma cell lines induced by β-escin through mitochondrial caspase-dependent pathway. *Phytother Res* 2011;25(10):1519-1526.

12 Tan SM, Li F, Rajendran P, Kumar AP, Hui KM, Sethi G. Identification of beta-escin as a novel inhibitor of signal transducer and activator of transcription 3/Janus-activated kinase 2 signaling pathway that suppresses proliferation and induces apoptosis in human hepatocellular carcinoma cells. *J Pharmacol Exp Ther* 2010;334(1):285-293.

13 Kasibhatla S, Tseng B. Why target apoptosis in cancer treatment? *Mol Cancer Ther* 2003;2(6):573-580.

14 Algeciras-Schimnich A, Shen L, Barnhart BC, Murmann AE, Burkhardt JK, Peter ME. Molecular ordering of the initial signaling events of CD95. *Mol Cell Biol* 2002;22(1):207-220.

15 Guo HR, Chen L, Cui HM, Peng X, Fang J, Zuo ZC, Deng JL, Wang X, Wu BY. Research advances on pathways of nickel-induced apoptosis. *Int J Mol Sci* 2015;17(1):E10.

16 Bhola PD, Letai A. Mitochondria-Judges and executioners of cell death sentences. *Mol Cell* 2016;61(5):695-704.

17 Piao SZ, Kang MY, Lee YJ, Choi WS, Chun YS, Kwak C, Kim HH. Cytotoxic effects of escin on human castration-resistant prostate cancer cells through the induction of apoptosis and G2/M cell cycle arrest. *Urology* 2014;84(4):982.e1-982.e7.

18 Gordon EM, Ravicz JR, Liu S, Chawla SP, Hall FL. Cell cycle checkpoint control: the cyclin G1/Mdm2/p53 axis emerges as a strategic target for broad-spectrum cancer gene therapy-a review of molecular mechanisms for oncologists. *Mol Clin Oncol* 2018;9(2):115-134.

19 Chao HX, Poovey CE, Privette AA, Grant GD, Chao HY, Cook JG, Purvis JE. Orchestration of DNA damage checkpoint dynamics across the human cell cycle. *Cell Syst* 2017;5(5):445-459.e5.

20 Niu YP, Wu LM, Jiang YL, Wang WX, Li LD. Beta-escin, a natural triterpenoid saponin from Chinese horse chestnut seeds, depresses HL-60 human leukaemia cell proliferation and induces apoptosis. *J Pharm Pharmacol* 2008;60(9):1213-1220.

21 Zhou XY, Fu FH, Li Z, Dong QJ, He J, Wang CH. Escin, a natural mixture of triterpene saponins, exhibits antitumor activity against hepatocellular carcinoma. *Planta Med* 2009;75(15):1580-1585.

22 Yuan SY, Cheng CL, Wang SS, Ho HC, Chiu KY, Chen CS, Chen CC, Shiau MY, Ou YC. Escin induces apoptosis in human renal cancer cells through G2/M arrest and reactive oxygen species-modulated mitochondrial pathways. *Oncol Rep* 2017;37(2):1002-1010.

23 Cheong DHJ, Arfuso F, Sethi G, Wang LZ, Hui KM, Kumar AP, Tran T. Molecular targets and anti-cancer potential of escin. *Cancer Lett* 2018;422:1-8.

24 Çiftçi GA, Işcan A, Kutlu M. Escin reduces cell proliferation and induces apoptosis on glioma and lung adenocarcinoma cell lines. *Cytotechnology* 2015;67(5):893-904.

25 Yang Y, Xue K, Li Z, Zheng W, Dong WJ, Song JZ, Sun SJ, Ma TH, Li WZ. c-Myc regulates the CDK1/cyclin B1 dependent G2/M cell cycle progression by histone H4 acetylation in Raji cells. *Int J Mol Med* 2018;41(6):3366-3378.

26 Braun F, de Carné Trécesson S, Bertin-Ciftci J, Juin P. Protect and serve: Bcl-2 proteins as guardians and rulers of cancer cell survival. *Cell Cycle* 2013;12(18):2937-2947.

27 Youle RJ, Strasser A. The BCL-2 protein family: opposing activities that mediate cell death. *Nat Rev Mol Cell Biol* 2008;9(1):47-59.

28 Juin P, Geneste O, Gautier F, Depil S, Campone M. Decoding and

unlocking the BCL-2 dependency of cancer cells. *Nat Rev Cancer* 2013;13(7):455-465.

29 Zhao ZQ, Velez DA, Wang NP, Hewan-Lowe KO, Nakamura M, Guyton RA, Vinten-Johansen J. Progressively developed myocardial apoptotic cell death during late phase of reperfusion. *Apoptosis* 2001;6(4):279-290.

30 Tait SW, Green DR. Mitochondria and cell death: outer membrane permeabilization and beyond. *Nat Rev Mol Cell Biol* 2010;11(9):621-632.

31 Li LY, Luo X, Wang X. Endonuclease G is an apoptotic DNase when released from mitochondria. *Nature* 2001;412(6842):95-99.

32 Li P, Nijhawan D, Budihardjo I, Srinivasula SM, Ahmad M, Alnemri ES, Wang X. Cytochrome c and dATP-dependent formation of Apaf-1/caspase-9 complex initiates an apoptotic protease cascade. *Cell* 1997;91(4):479-489.

33 Pradelli LA, Bénéteau M, Ricci JE. Mitochondrial control of caspase-dependent and -independent cell death. *Cell Mol Life Sci* 2010;67(10):1589-1597.

34 Kroemer G, Reed JC. Mitochondrial control of cell death. *Nat Med* 2000;6(5):513-519.

35 Green DR, Reed JC. Mitochondria and apoptosis. *Science* 1998;281(5381):1309-1312.

36 Lochmann TL, Bouck YM, Faber AC. BCL-2 inhibition is a promising therapeutic strategy for small cell lung cancer. *Oncoscience* 2018;5(7-8):218-219.

37 Baig S, Seevasant I, Mohamad J, Mukheem A, Huri HZ, Kamarul T. Potential of apoptotic pathway-targeted cancer therapeutic research: where do we stand? *Cell Death Dis* 2016;7:e2058.

38 Hengartner MO. The biochemistry of apoptosis. *Nature* 2000;407(6805):770-776.

39 Lin PY, Tsai CT, Chuang WL, Chao YH, Pan IH, Chen YK, Lin CC, Wang BY. Chlorella sorokiniana induces mitochondrial-mediated apoptosis in human non-small cell lung cancer cells and inhibits xenograft tumor growth *in vivo. BMC Complement Altern Med* 2017;17(1):88.

40 Jing ZT, Liu W, Wu SX, He Y, Lin YT, Chen WN, Lin XJ, Lin X. Hepatitis B virus surface antigen enhances the sensitivity of hepatocytes to fas-mediated apoptosis via suppression of AKT phosphorylation. *J Immunol* 2018;201(8):2303-2314.